ACS Sustainable Chemistry & Engineering

Research Article

pubs.acs.org/journal/ascecg

Value-Added Chemicals from Microalgae: Greener, More Economical, or Both?

Jian Gong and Fengqi You*

Department of Chemical and Biological Engineering, Northwestern University, 2145 Sheridan Road, Evanston, Illinois 60208, United States

Supporting Information

ABSTRACT: This paper addresses the sustainable design and synthesis of manufacturing processes for making algal bioproducts. We propose by far the most comprehensive superstructure capable of producing biodiesel, hydrogen, propylene glycol, glycerol-*tert*-butyl ether, and poly-3-hydroxybutyrate from microalgae. The major processing sections include cultivation, harvesting, lipid extraction, remnant treatment, biogas utilization, biofuel proneduction, and bioproduct manufacturing. On the basis of the superstructure, we integrate a cradle-to-gate life cycle analysis and techno-economic analysis with multiobjective optimization to simultaneously optimize the environmental and economic performance. We also apply a tailored global optimization algorithm to efficiently solve the problem in reasonable computation times. Results show that the most environmentally sustainable processes reduce life cycle greenhouse gas emissions per kilogram of the algal bioproducts by 5% to 63%, compared with petrochemical counterparts. In addition, the coproduction of value-added bioproducts in the algal glycerol process helps reduce the biodiesel production cost to as low as $2.79 per gasoline-gallon-equivalent.

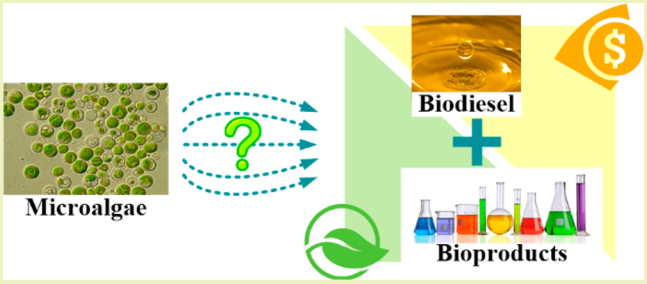

KEYWORDS: *Life cycle analysis, glycerol, bioproduct, algal biofuels, global optimization*

INTRODUCTION

Each year, over 15% of the petroleum consumed in the United States is converted to 900 million tons of chemicals, or 90% of the total chemicals market.[1−6] Due to the fact that most synthesis processes for fossil-derived chemicals are energy- and emissions-intensive, in contrast, sustainable bioproducts converted from biomass offer attractive substitutes with fewer environmental impacts.[7−9] From an economic standpoint, lab-scale designs for emerging advanced biofuel production technologies commonly encounter economic challenges during scale-up, diminishing the commercial viability of an environmentally sustainable process design. In addition to the ongoing research into the productivity of an effective operation, it would be beneficial to produce value-added bioproducts along with biofuels from a systematic perspective. For instance, as a result of the continually expanding biodiesel industry, surplus glycerol produced from the transesterification reaction depresses the glycerol price to a very low level. Fortunately, glycerol is a versatile building block chemical, and the conversion of glycerol to its value-added derivatives, rather than selling raw glycerol to the market, offers an opportunity to relieve the increasing environmental pressure and reduce the biodiesel price simultaneously.[10−12]

Among a wide array of biomass feedstocks, microalgae have recently received substantial attention in both academia and industry owing to their potential for a high lipid accumulation rate and minimum competition with food and crops.[13,14] There are a few existing publications that offer insights into the sustainable design and synthesis of algal systems. Gebreslassie et al. proposed a detailed superstructure of an algal biorefinery for biofuel production.[15] Despite a large number of technology alternatives included, they focused primarily on the production of algal biofuels, and did not exploit the potential environmental and economic benefits from value-added bioproducts. To explore algal biorefinery processes with better economics, Gong et al. optimized the performance of algal biorefinery processes for biological carbon sequestration and utilization.[16] However, the upgrading technology was restricted to hydroprocessing for the production of "drop-in" renewable diesel, and did not consider the utilization of byproducts. Martin and Grossmann optimized the coproduction of biodiesel and glycerol ethers from algae oil,[17] but little attention was paid to environmental impacts, and glycerol derivatives were limited to glycerol ethers. Rizwan et al. proposed a superstructure to quickly scan through the algal processing pathways and identify the optimal routes with respect to various objective functions;[18] however, their discussion did not cover the value-added bioproducts from glycerol, and no environmental performance was included. An algal biorefinery integrated with a steam electric power plant was reported to be profitable at current

Received: September 10, 2014
Revised: November 25, 2014
Published: December 8, 2014

biodiesel prices,[19] which could be even more affordable if the glycerol was further upgraded. In addition to superstructure optimization, Silva et al. simulated an algae-to-biodiesel process with a biodiesel price of $4.34/gallon, which is too high to be attractive from the economic perspective.[20] Pokoo-Aikins et al. concluded algal biodiesel is competitive with food-based plant oil.[21] Additionally, much effort was also made on sustainable design and synthesis of thermochemical conversion system,[22−27] offering useful ideas for the integration of energy systems. Even with the above progress, there still lacks a complete superstructure which not only incorporates existing technologies for the conversion of algal biodiesel, but also takes advantage of the versatile glycerol and converts it on site to environmentally sustainable and value-added bioproducts. Process integration is an important method in sustainable process design to explore the possibilities of improving the overall process efficiency by utilizing waste streams and ultimately reduce the overall expenditure and environmental impacts of the entire process. Bioproduct manufacturing has the potential for boosting the algal biodiesel performance by utilizing byproducts in transesterification and generating carbon dioxide feed for microalgae growth. The aim of the current work, therefore, is to explore the potential environmental and economic benefits for the production of both biodiesel and value-added bioproducts from microalgae.

To bridge the research gap, we have developed by far the most comprehensive superstructure, which is able to produce biodiesel and four types of bioproducts, including hydrogen, propylene glycol (PG), glycerol-*tert*-butyl ether (GE), and poly-3-hydroxybutyrate (PHB). In particular, the hydrogen can be produced by steam reforming, autothermal reforming, or aqueous-phase reforming. The superstructure also includes a methanol synthesis process (see the Biogas Utilization section). Additionally, we simulate the lipid extraction processes using hexane and *n*-butanol as extractants for data validation. Based on the proposed superstructure, a cradle-to-gate life cycle analysis (LCA) is performed to account for the life cycle greenhouse gas (GHG) emissions associated with three life cycle stages, namely feedstock acquisition, transportation, and algal biodiesel and bioproduct manufacturing. Following a life cycle optimization methodology, we further integrate the LCA and techno-economic analysis with multiobjective optimization to simultaneously optimize the environmental and economic performance. A tailored global optimization algorithm is applied to circumvent the computational difficulties caused by separable concave terms and mixed integer fractional terms in the objective functions. The results from this study justify the significance of manufacturing bioproducts in algal biodiesel processes and offer guidance to related technology advancement.

The rest of this paper is organized as follows. The process description is presented in the next section, followed by a brief explanation of a cradle-to-gate LCA. Necessary information on the optimization problem is provided in the Problem Statement section. Later, we propose a multiobjective mixed-integer nonlinear programming (MINLP) model and the global optimization strategy for efficient computation. In the next section, we discuss the LCA results, economic performance, and the computational comparison. The paper is concluded in the last section.

EXPERIMENTAL SECTION

Process Description. A process superstructure refers to a collection of process alternatives that are candidates for a feasible or optimal design.[28] In this work, we propose by far the most comprehensive superstructure for the production of biodiesel and bioproducts from the microalgae strain *Chlorella vulgaris*, as illustrated in Figure 1. The superstructure can be divided into seven sections: cultivation, harvesting, lipid extraction, remnant treatment, biogas utilization, biofuel production, and bioproduct manufacturing. The details of each section of the superstructure are given in the following subsections.

Cultivation. Given a carbon source, nutrients, and water, a commonly cultivated microalgae strain, *Chlorella vulgaris* (nitrogen starvation may significantly increase the lipid content, but a widely used 25 wt % lipid content is applied in this work), is flourished in raceway open ponds (Figure 2). As shown in Table S27 (in the Supporting Information), the carbon dioxide concentration in the carbon source is 21.14%, which falls in the range of healthy growth of microalgae.[29] Algal biodiesel and bioproducts are considered environmentally beneficial because waste carbon dioxide generated in the process can utilized by microalgae as extra carbon source. Enlightened by this idea, we recycle the off-gas streams to the open ponds instead of releasing them to the environment. One kilogram of carbon dioxide consumed contributes to 0.526 kg of microalgae.[30] However, it is impossible for microalgae to capture and digest the entire input carbon source in a single-pass injection. Due to the difficulty of collecting emitted gas from the open ponds, as much as 25% of the carbon

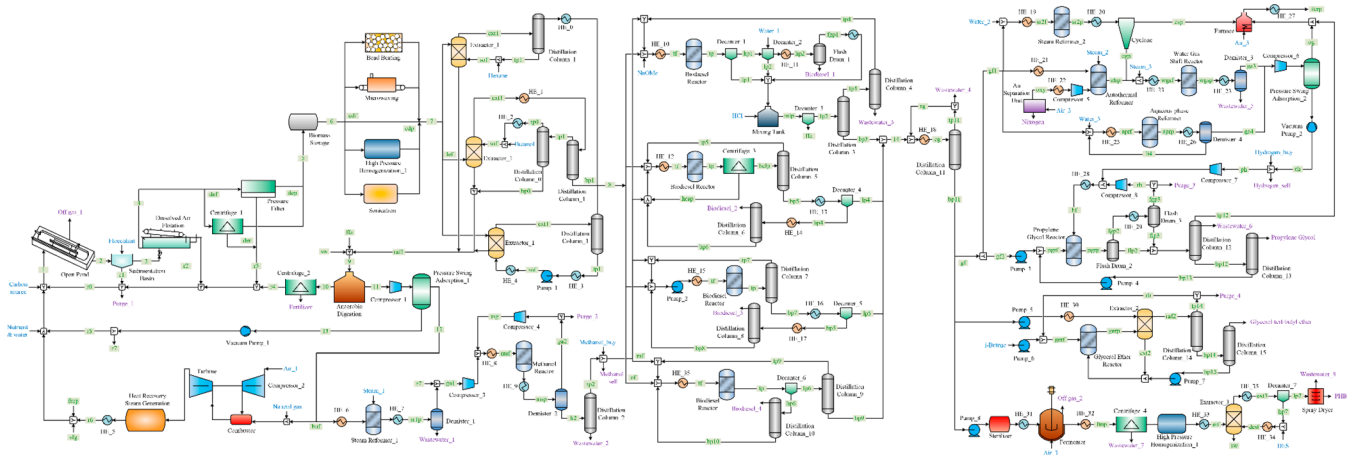

Figure 1. Proposed superstructure for the production of bioproducts and biofuel. Blue, purple, and green streams represent system input, system output, and connecting streams, respectively.

dx.doi.org/10.1021/sc500683w | ACS Sustainable Chem. Eng. 2015, 3, 82−96

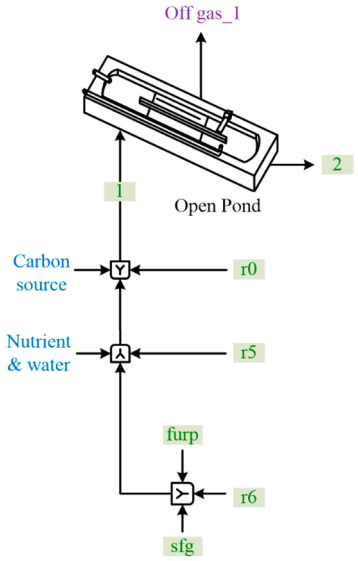

Figure 2. Process diagram of the cultivation section.

dioxide together with the oxygen produced during photosynthesis is expelled to the environment.[30]

Harvesting. Containing only 0.015 wt % of mature biomass, the immediate product from the open ponds is unable to be handled and utilized by downstream technologies. Therefore, as shown in Figure 3, we employ a three-step strategy in the Harvesting section to reduce the undesired water content. The first equipment unit is a sedimentation basin, which separates most of the surplus water from the dilute product via autoflocculation and achieves a concentration of 1 wt %.[31] The flocculant added to assist gravitational separation is a type of cationic polyelectrolyte and the effective concentration is 3×10^{-6} according to existing experimental results.[32] We assume the impact of the flocculant on the downstream processing is negligible due to the small quantity. The second step involves the use of a dissolved air flotation system, which increases the algal concentration to 10 wt %.[33] Finally, the algae slurry is processed by one of the two technology alternatives: pressure filtration and centrifugation. Both technologies can thicken the algae slurry to 30 wt %,[34,35] but pressure filtration consumes less energy, whereas a centrifuge is less expensive to install. A total of 5 wt % of the separated water is purged, while the remaining is recycled to the open ponds. As discussed previously, the equipment in the Cultivation and Harvesting sections operate only during daytime because sun light is one of the necessary ingredients for the algae growth. Therefore, a biomass storage tank to store 50% of biomass is employed at the end of the Harvesting section so that the downstream processes receive biomass feed continuously throughout the day. Inoculation is not considered in this supersturcure.

Lipid Extraction. Because lipid materials, in the form of fatty acids and triacylglycerols, are mixed in the algal cells with other components, such as proteins and carbohydrates, solvent extraction is applied to separate these convertible lipids. Before sending the algal biomass directly to extractors, it should be noted that the inclusion materials are protected by cell membranes and cell walls, which may to some extent inhibit the effective contact between the extractant and the target lipids. Following the results from Lee,[36] we consider five cell disruption methods in the superstructure to improve the efficacy of the solvent extraction system. In Figure 4, bead beating, microwaving, high pressure homogenization, and sonication are four energy-intensive cell disruption methods with various disruption effects. The last option is to bypass the cell disruption, which lowers the lipid content available for extraction, but avoids the exceeding energy consumption. The mass balance model of this section is shown in eqs S20−S39 (Supporting Information) and corresponding data are listed in Tables S19 and S20 (Supporting Information).

The extraction technologies considered in this work belong to wet extraction, which avoids the intensive energy consumption in drying the microalgae to powders. Most existing research regarding lipid extraction is limited to finding appropriate solvents at the laboratory scale,[37] but these experimental results might be less attractive and profitable when they are embedded in a complete process. For instance, butanol is a commonly available solvent with a good lipid extraction yield and little side effect to most downstream processes, but the butanol recovery step consumes a large amount of utilities due to the existence of water. In this work, we consider using solvent extraction to separate lipids from wet algal paste without completely drying the biomass. Three chemicals, namely hexane, n-butanol, and supercritical carbon dioxide, are considered as alternative solvents in the lipid extraction. Because of a lack of justified data of complete extraction-recovery cycles for hexane and n-butanol, the processes for these solvents are constructed and simulated using Aspen Plus.[38] Screenshots of the Aspen Plus processes can be found in Figures S1 and S2 in the Supporting Information.

Hexane is not miscible in water, so only one distillation column is necessary to partition lipid and the solvent. In contrast, butanol is soluble in water and at least two distillation columns are needed if the solvent is to be reused. As a result of the large amount of energy spent on separating water and alcohol, lipid extraction by butanol loses its significant advantage in a complete extraction-solvent recovery system. The cursory analyses are concluded from the simulation results as listed in Table 1. The data for supercritical carbon dioxide extraction is retrieved from the literature.[39,40]

Remnant Treatment. Despite the significance of algal lipids in biofuel conversion, they only contribute to as much as 25 wt % of the dry biomass. In fact, a substantial proportion of the energy captured by algae still remains in the lipid-extracted algal cells, or algal remnant. In the proposed superstructure (detailed by Figure 5), algal remnant is introduced into digesters, where long chain organic molecules are decomposed into short chain carbon dioxide and methane by active anaerobic bacteria. Methane is carefully purified from the waste carbon

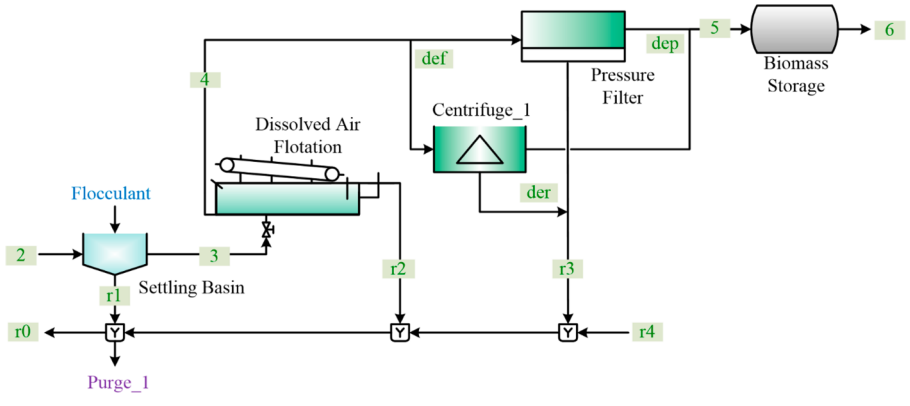

Figure 3. Process diagram of the harvesting section.

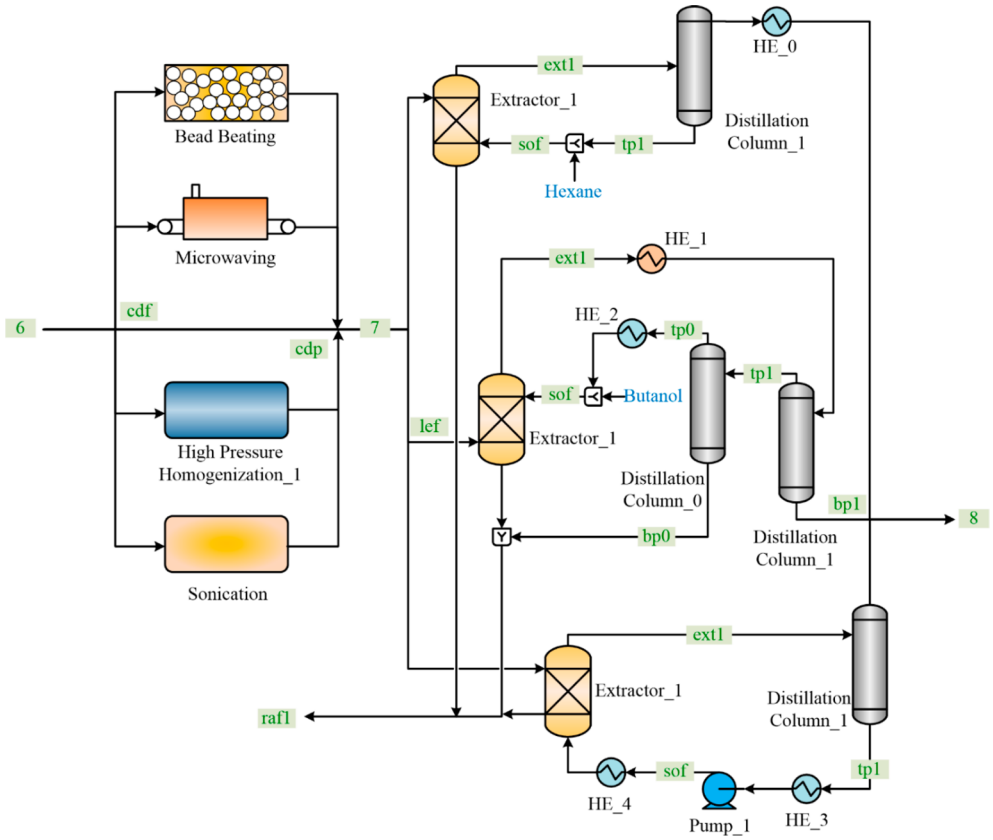

Figure 4. Process diagram of the lipid extraction section. HE represents heat exchanger.

Table 1. Simulation Results for Hexane Extraction and *n*-Butanol Extraction

hexane extraction	stream ext1	mass flow rate of lipid	43.75	kg/h
		mass flow rate of water	0	kg/h
		mass flow rate of solvent	1000	kg/h
	distillation column DC1	top temperature	345	K
		bottom temperature	420	K
		heat duty	0.2	MW
		cold duty	0.19	MW
		capital cost	0.37	$MM
n-butanol extraction	stream ext1	mass flow rate of lipid	6684	kg/h
		mass flow rate of water	5044	kg/h
		mass flow rate of solvent	24160	kg/h
	distillation column DC1	top temperature	380	K
		bottom temperature	459	K
		heat duty	17.23	MW
		cold duty	15.63	MW
		capital cost	0.77	$MM
	distillation column DC0	top temperature	383	K
		bottom temperature	403	K
		heat duty	44.29	MW
		cold duty	43.84	MW
		capital cost	1.42	$MM

dioxide through a pressure-swing-adsorption system. Simultaneously, important elements like nitrogen and phosphorus are released to the effluent and reused in algae cultivation after solid fertilizers are separated by centrifugation.

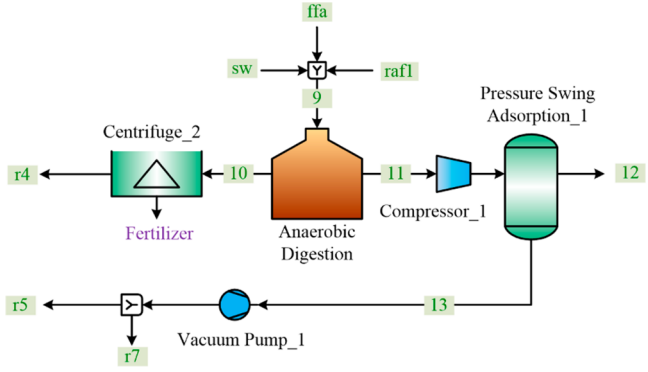

Figure 5. Process diagram of the remnant treatment section.

Biogas Utilization. To fully exploit the methane from anaerobic digestion, two methods are considered: on-site power generation and methanol synthesis. If power generation is chosen (left in Figure 6), the fuel gas is sent to a combustor, and the corresponding flue gas enters a turbine and a heat recovery steam generation system sequentially, resulting in an overall energy-to-electricity conversion of 58% on the basis of lower heating values of the combustible gases.[30] Otherwise, if methanol synthesis is selected, the methane feed is introduced into a reformer together with steam, and converted into carbon monoxide and hydrogen. Dried by a demister, the syngas product is enriched by a carbon dioxide stream and converted to methanol. Finally, methanol, wastewater, and unreacted gases are obtained from two distillation columns. A small proportion of the unreacted gases are purged to a furnace, while the remaining are recycled to the methanol reactor. In case that the methanol is more than the downstream demand or no methanol is produced in this section, we allow methanol to be sold to or purchased from the market. The possibility of buying and selling methanol simultaneously is eliminated by employing the binary variable as in eqs S69 and S70 in the Supporting Information.

dx.doi.org/10.1021/sc500683w | ACS Sustainable Chem. Eng. 2015, 3, 82−96

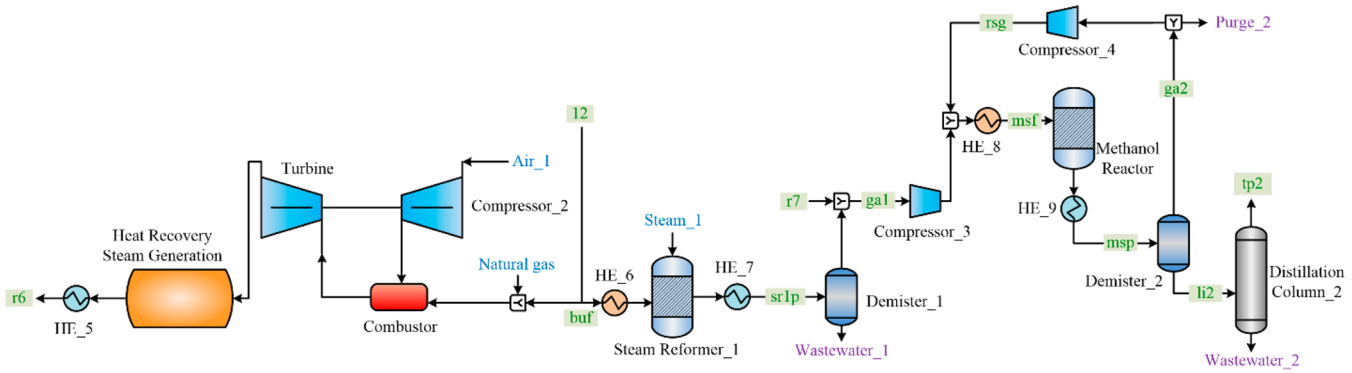

Figure 6. Process diagram of the biogas utilization section.

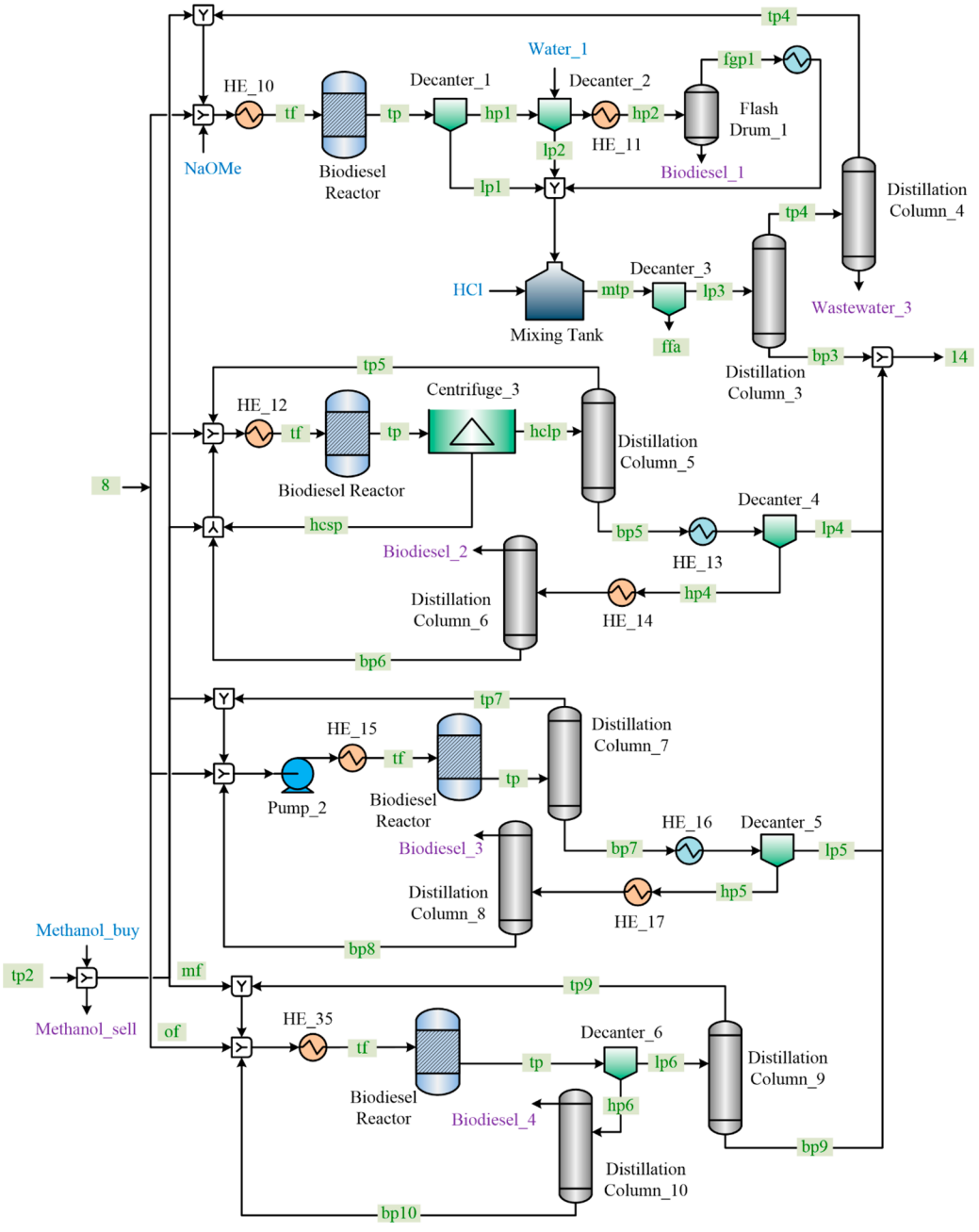

Figure 7. Process diagram of the biofuel production section.

Biofuel Production. Many of studies have focused on transesterification of lipids from biomass resources and various reaction conditions have been tested and simulated.[41,42] In Figure 7, four transesterification technologies are considered, namely, sodium

dx.doi.org/10.1021/sc500683w | ACS Sustainable Chem. Eng. 2015, 3, 82−96

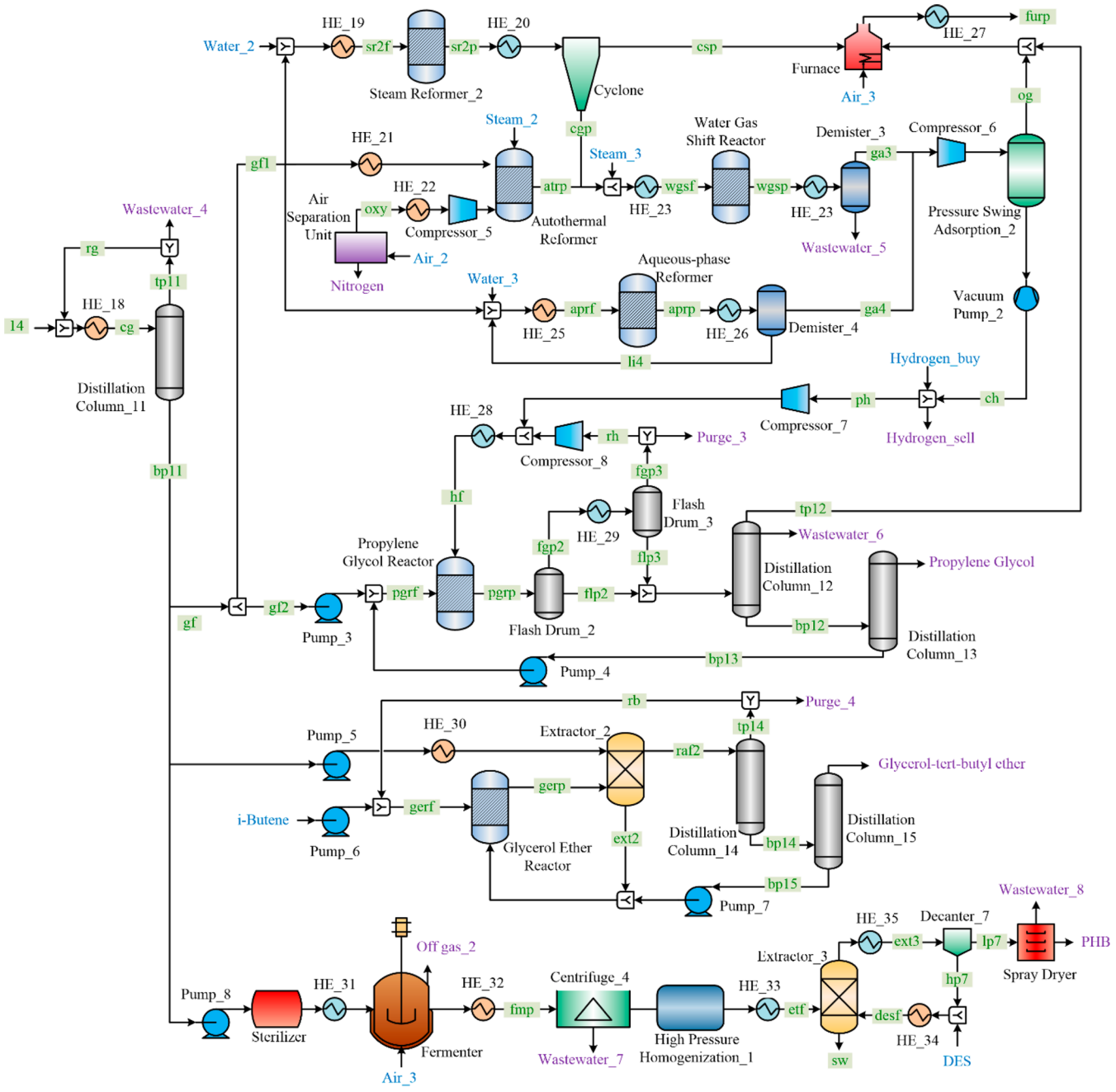

Figure 8. Process diagram of the bioproduct manufacturing section.

methoxide-catalyzed transesterification,[43] heterogeneously catalyzed transesterification,[44] enzyme-catalyzed transesterification,[45] and supercritical methanol transesterification.[44] Whatever technology selected, the core reaction involves transforming one molecule of triglyceride to one molecule of glycerol and three molecules of fatty acid alkyl esters, or biodiesel. Although methanol is commonly regarded as the other reactant in transesterification, short chain alcohol chemicals, like ethanol, propanol, and butanol, are able to complete the same reaction. Therefore, we assume that butanol residue from the lipid extraction section undergoes transesterification with priority. Once the butanol runs out, or no butanol is mixed in the lipid feed, methanol is introduced and continues the reaction until the lipids run out.

Bioproducts Manufacturing. The immediate products from the biofuel production section are biodiesel and glycerol with an approximate weight ratio of 10:1. Glycerol is an important platform chemical which can be upgraded to value-added chemicals through selective oxidation, etherification, hydrogenolysis, dehydration, reforming, carbonate, epichlorohydrin, etc.[11] In this work, we consider the conversion of purified glycerol from microalgae to four types of bioproducts, including hydrogen, PG, GE, and PHB. The process flow diagram of this section is shown in Figure 8.

Hydrogen. Yielding only water during oxidation, hydrogen is regarded as a clean and efficient fossil fuel substitute.[46] Furthermore, it participates in some important industrial reactions, like hydrotreating and hydrocracking.[47] Motivated by these merits, researchers attempted to produce hydrogen from various feedstocks, including surplus glycerol from biodiesel production, and through a plethora of technologies, including gasification, pyrolysis, catalytic steam reforming, and so forth.[46,48] In this work, we investigate hydrogen production from purified glycerol via three different methods: steam reforming, autothermal reforming, and aqueous-phase reforming.

In the first method, purified glycerol and water are sent to a steam reformer at 565 °C and converted to carbon monoxide, hydrogen, methane, ethylene, and char.[49,50] The feed glycerol is heated to 565 °C

dx.doi.org/10.1021/sc500683w | ACS Sustainable Chem. Eng. 2015, 3, 82−96

by a heat exchanger based on the values reported by Jones et al.[47] As an endothermic reaction, glycerol steam reforming extracts heat from the furnace, where all the purged gases are burned. The solid char is eliminated from the reaction products via a cyclone, while the remaining gases and a stream of steam are injected into a water−gas-shift reactor, where most of the carbon monoxide and water are converted to carbon dioxide and hydrogen.[51] After surplus water is separated by a demister, the gas products undergo pressure swing adsorption to obtain a hydrogen stream with 99 wt % purity. As also assumed by Jones et al.,[47] the 1% impurities primarily consist of carbon dioxide which does not influence the propylene glycol production.

Hydrogen production via autothermal reforming of glycerol is able to achieve a net zero energy consumption by appropriately combining the endothermic reforming reaction and the exothermic oxidation of glycerol.[52] Regarding the oxidation reaction, the consumed oxygen is produced on site by an air separation unit, whose byproduct, nitrogen, can be sold to the market.[53] Next, gas products are sent to a water−gas-shift reactor, a demister, and a pressure-swing-adsorption system sequentially in a similar fashion to steam reforming.

The last hydrogen production technology is aqueous-phase reforming. As reported by Guo et al.,[54] this reforming reaction takes place under a relatively mild temperature of 225 °C in the presence of a Ni−B amorphous alloy catalyst, but achieves a single loop conversion of only 9%. Large amounts of unreacted glycerol and water are recycled from a demister to the inlet of the reactor. Because the hydrogen selectivity is already high in aqueous-phase reforming, the gas products bypass the energy intensive water−gas-shift reaction for hydrogen enrichment, and undergo a pressure-swing-adsorption system for hydrogen purification directly after the demister.

Propylene Glycol. PG, or 1,2-propanediol, commonly produced by propylene oxidation, serves as an important feedstock of unsaturated polyester resins.[55] As opposed to the conventional route, PG is produced through catalytic hydrogenolysis of glycerol in the present superstructure. Glycerol and hydrogen react at 190 °C and become a mixture of water, PG, propanol, acetone, and unreacted glycerol and hydrogen. Two flash drums are employed sequentially to separate unreacted hydrogen from the other products, and 5% of the gas materials are purged to the furnace.[56,57] Next, 99.5 wt % PG product is achieved by using two distillation columns to separate waste and unreacted materials from the product.

Glycerol-tert-butyl Ether. Another important group of glycerol derivatives are GEs. Specifically, di*tert*-butyl glycerol ether (DE) and tri*tert*-butyl glycerol ether (TE) are very useful additives to diesel fuels due to their antidetonant and octane-enhancing nature.[55] Additionally, they are able to reduce the emissions of fumes, particulates, and carbon oxides resulting from fuel combustion. In this work, a mixture of DE and TE can be produced following the purification of crude glycerol.

Besides glycerol, the other important raw material for GE production is isobutylene, which is mixed with 10 wt % isobutane. The etherification reaction takes place at 90 °C and 1.4 MPa.[58] Both the feed and the products maintain their liquid states under such conditions. Before being sent to the reactor, the purified glycerol is regarded as an extractant to separate most of the unreacted glycerol and mono*tert*-butyl glycerol ether from the etherification reaction. Next, the raffinate is introduced into a distillation column where unreacted isobutylene and isobutane are separated from the top of the column and recycled to the reactor after a small amount is purged. The remaining products undergo distillation again and become qualified products.

Poly-3-hydroxybutyrate. As a group of polyhydroxyalkanoates, PHB's are attractive biodegradable substitutes for conventional petroleum-derived plastics and can be upgraded to fibers, films, and heteropolymers.[59] According to Posada et al.,[60] PHBs can be synthesized by *Cupriavidus necator* JMP 134 over a glycerol-based substrate. In the PHB process, the sterilized glycerol is sent into a fermentation reactor with abundant air. The fermentation reaction converts glycerol to water, carbon dioxide, intracellular PHB, and other cell building materials, which are regarded as remnant. Next, a centrifuge is employed to reduce the water content in the fermentation products. After cell disruption by high pressure homogenization, the concentrated biomass is sent to an extractor so that the PHB product can be extracted by diethyl-succinate (DES). The raffinate is sent to anaerobic digestion for energy recovery, while the extracts are introduced to a decanter after being cooled to 25 °C by a heat exchanger. The PHB product in the light phase is further dried by a spray drier, and DES solvent in the heavy phase is reused.

Life Cycle Analysis and Optimization. The goal of this study is to quantitatively determine the minimum life cycle environmental impacts of the bioproducts and biodiesel from microalgae. The functional unit of this LCA is defined as 1 kg of bioproduct manufactured, following the definitions by Rostkowski et al.[61] In this work, the impact category to assess the life cycle environmental performance of manufacturing bioproducts and biodiesel from microalgae is dedicated to global warming. The corresponding environmental metric, GWP, is calculated using the IPCC (International Panel on Climate Change) method with characterization factors of a 100-year horizon (GWP 100a).[62]

System Boundaries. Refined from the proposed superstructure, the system boundaries for the LCA are illustrated with major processing blocks, emissions, and input and output materials in Figure 9. As a process-based LCA, the system boundaries take into consideration the life cycle GHG emissions associated with three life cycle stages, namely, feedstock acquisition, transportation, and algal biodiesel and bioproduct manufacturing. The direct emissions in the algal biodiesel and bioproduct manufacturing stage include off-gas released in the Cultivation section and wastewater throughout the entire process. The indirect emissions account for life cycle GHG emissions associated with electricity, heating, and cooling utilities consumed in the process. Due to the lack of information about the end-of-life phases of several nonfuel chemicals, the LCA is confined to a "cradle-to-gate" analysis. We also assume that the carbon dioxide source comes from a nearby coal-fired power plant and water is also available in nearby sources. As a result, the environmental impacts associated with flue gas acquisition and transportation, as well as water transportation, are excluded from this analysis.[63,64] Furthermore, life cycle GHG emissions associated with materials and energy consumed in construction of the processes are also excluded.[65]

Data Source. The LCA in this work is based on mass and energy balances of the comprehensive superstructure. We make our attempts to find and organize the most up-to-date data available in the literature. Data selection is prioritized to U.S. databases, such as electricity prices and average transportation distances. Process data related to mass and energy balances, as well as parameters for economic evaluation, are extracted from literature and Aspen Plus simulation results.[38] The distances for delivering various feedstocks to the algal biorefinery are assumed to be the average U.S. transportation values specified by commodity categories,[66] while the life cycle impact assessment parameters for translating the mass of various materials, energy consumption, and transportation quantity (measured by the product of distance and mass of the feedstock) to corresponding GWP contributions are taken from the EcoInvent database.[67] Please refer to Table S30 in the Supporting Information for detailed life cycle inventory data.[14,30,33,35,68,69]

Coproduct Allocation. There are several potential coproducts in addition to bioproducts (hydrogen, PG, GE, and PHB) and biodiesel in the superstructure, namely, fertilizer from anaerobic digestion, methanol and electricity from biogas utilization, and nitrogen and hydrogen from hydrogen production. According to the ISO guidelines,[70] we treat the surplus electricity as an environmental credit and subtract the corresponding environmental impact from the total GWP. Next, a portion of the electricity-modified total GWP is allocated to each coproduct based on its economic value when leaving the system boundaries.

Life Cycle Optimization. Some metrics are developed to quantitatively evaluate a process. For instance, the environmental impact can be quantified by the total GWP, whereas the economic performance of a process can be evaluated by the total annualized cost (TAC).[68] Commonly, life-cycle and techno-economic analyses require predefined processes and systems, therefore lacking the ability to generate feasible process designs from a process superstructure with better or best process performance (e.g., economics and environmental sustainability). In this work, an integrated methodology termed

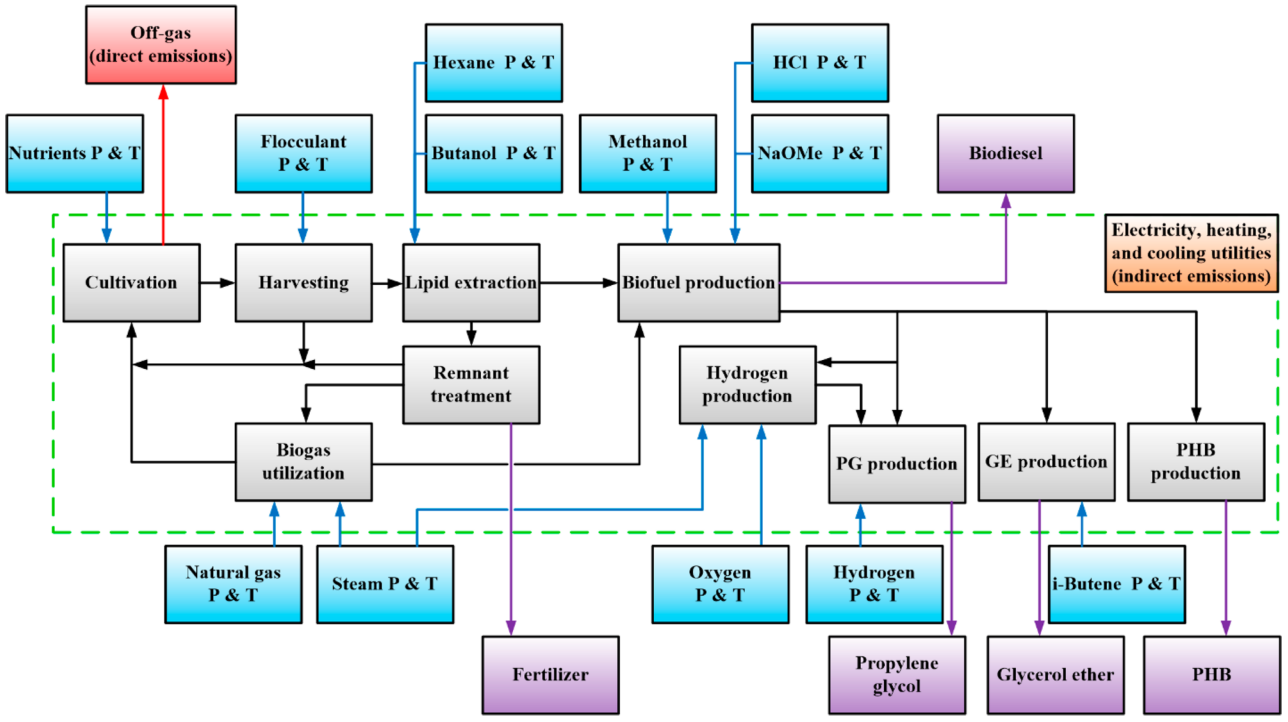

Figure 9. System boundaries of a cradle-to-gate LCA for the production of biodiesel and bioproducts from microalgae include three life cycle stages: feedstock acquisition, transportation (denoted together by blue blocks), and algal biodiesel and bioproduct manufacturing (denoted by green dotted box). Direct and indirect GHG emissions in the manufacturing stage are represented with red and orange blocks, respectively. Major process operations and final products are denoted as gray and purple blocks, respectively. P&T, production and transportation.

life cycle optimization,[71−73] which enables the multiobjective optimization of a system under both economic and environmental criteria, is used to simultaneously optimize environmental and economic performances of manufacturing bioproducts and biodiesel from microalgae. This methodology requires establishing a rigorous equation-based multiobjective mathematical optimization model based on the proposed superstructure for manufacturing algal bioproducts and biodiesel. The problem statement, model formulation, and optimization algorithms are introduced in the following sections.

Problem Statement. In this life cycle optimization problem, the most comprehensive superstructure by far is developed for the production of algal bioproducts and biodiesel. The superstructure consists of seven sections and a variety of technology alternatives. Specifically, the cultivation section is established with raceway open ponds. The harvesting section encompasses a settling basin, a dissolved air flotation system, and either a pressure filter or a centrifuge in the end. The lipid extraction section is composed of a biomass storage tank, a cell disruption system with five technology alternatives, and three solvent extraction options. The remnant treatment section is made up of an anaerobic digester and a centrifuge, followed by a biogas utilization section where biogas is consumed either by combustion or methanol synthesis. The biofuel production section employs four transesterification technology alternatives to produce biodiesel, and the last bioproduct manufacturing section could synthesize hydrogen with three technologies, PG, GE, and PHB.

The mass flow rate of the feed carbon source is fixed. Physical properties of feed and product materials are given, including, but not limited to, species distributions of nutrients, flocculant, natural gas, steam, hexane, n-butanol, methanol, sodium methoxide, hydrochloric acid, oxygen, hydrogen, isobutylene, and DES. Additionally, we are given product distributions and conversions of microalgae cultivation, anaerobic digestion, combustion of organic materials, steam reforming reactions of biogas and glycerol, transesterification, water−gas-shift reaction, and synthesis reactions for methanol, PG, GE, and PHB. Operating temperatures and pressures of all operations as well as split fractions of separation units are known. Unit power, heating, or cooling utility consumption, or temperature differences and efficiency of heat-exchanging equipment are available in the literature. We are also given parameters pertaining to economic evaluation including life span of the biorefinery, interest rate, sizing factors, base-case costs and mass flow rates, chemical engineering plant cost indices, capital-to-investment parameter, and prices of feed materials and products. For the purpose of the LCA, transportation distances and damage factors for GWP calculations are known.

The aim of this optimization model is to determine the most sustainable strategy of producing value-added bioproducts and biodiesel. Decision variables of this multiobjective optimization problem include technology selections in harvesting, lipid extraction, biogas utilization, biofuel production, and bioproduct manufacturing, mass flow rates of all streams, power, heating, or cooling utility consumption or generation of different equipment, equipment capital cost, operating cost, and GWP's for feedstock acquisition, transportation, and algal biodiesel and bioproducts manufacturing.

Model Formulation and Solution Method. A bicriteria MINLP model is formulated to optimize the design and operation of algal biodiesel and bioproducts manufacturing processes. This model consists of an environmental objective function, an economic objective function, and four types of constraints. In the mass balance constraints, the relationship between the input and output streams of a separation unit is developed based on the split fraction and mass conservation of every species (44 species are considered). The reactions are described with stoichiometric coefficients and conversions, or product distributions, depending on the type of data available in the literature. Also, integer variables are introduced to model technology selection decisions. The energy balance of each unit is closely related to the corresponding mass balance such that the electricity, heating, and cooling utility consumption are based on the mass flow rates of the input and output materials. The economic evaluation constraints calculate annualized investment cost based on equipment capital costs that follow a nonlinear scaling rule. These constraints also determine the annual operating cost, taken as the sum of feedstock cost, utility cost, operating and maintenance cost, and waste treatment cost. Finally, the TAC is calculated as the sum of the annualized investment cost and the annual operating cost. The constraints for life cycle

dx.doi.org/10.1021/sc500683w | ACS Sustainable Chem. Eng. 2015, 3, 82−96

environmental impact analysis first evaluate the life cycle GHG emissions originating from raw material acquisition, transportation, and algal biodiesel and bioproduct manufacturing. Next, the emissions are translated into environmental impacts, which are finally aggregated to the total GWP.

$$\begin{aligned}&\min \quad tac \text{ in S367}\\ &\min \quad gwp \text{ in S387}\\ &\text{s. t.} \quad \text{mass balance constraints S1}-\text{S207}\\ &\qquad \text{energy balance constraints S208}-\text{S317}\\ &\qquad \text{economic evaluation constraints S318}-\text{S367}\\ &\qquad \text{life cycle environmental impact analysis constraints S372}-\text{S387}\end{aligned} \tag{P1}$$

$$\begin{aligned}&\min \quad \frac{mtac}{v^{diesel}} \text{ in S371}\\ &\min \quad \frac{mgwp}{t} \text{ in S391}\\ &\text{s. t.} \quad \text{mass balance constraints S1}-\text{S207}\\ &\qquad \text{energy balance constraints S208}-\text{S317}\\ &\qquad \text{economic evaluation constraints S318}-\text{S371}\\ &\qquad \text{life cycle environmental impact analysis constraints S372}-\text{S391}\end{aligned} \tag{P2}$$

The bicriteria MINLP model consists of one environmental objective function and one economic objective function. Each objective function could optimize either total quantities or unit quantities. For instance, problem P1 minimizes total GWP and TAC simultaneously. Despite its common usage in design problems, minimizing total objective functions sometimes fails to reflect the competitiveness of a product, especially when the optimal solution achieves a slightly lower cost or environmental impact by significantly reducing the production.[73−75] Minimizing unit objective functions, however, considers both total behavior and the product quantity, thus providing an opportunity to directly and constructively compare the optimal results with real market values. To that end, the unit objective functions are associated with the functional unit of the LCA, the prevalent units on the real market, or the commonly used units in the literature. For instance, the environmental objective in problem P2 is to minimize the GWP per 1 MJ of energy of biodiesel produced,[64,76] and the corresponding economic objective is to minimize the TAC per gasoline gallon equivalent (GGE) of biodiesel produced.[24] In the objective functions of P2, the variable *mtac* represents the modified TAC by considering the byproducts as credits, v^{diesel} stands for the total volume of the biodiesel produced during a year, *mgwp* is the modified total GWP, which accounts for the allocation of surplus electricity, and the denominator t helps determine the unit GWP of algal biodiesel. The detailed MINLP model is provided in constraints S1−S391 in the Supporting Information and the related data are also given in Tables S1−S31 in the Supporting Information.

Both problems P1 and P2 are formulated as bicriteria, nonconvex MINLP's, which could be computationally demanding for general purpose solvers, due to their combinatorial and nonconvex nature. Therefore, several solution methods are applied to solving these problems. Regarding the objective functions, the ε-constraint method is applied to transfer the environmental objective function into a new ε-constraint.[77] For P1, the only nonlinear terms are the exponential sizing equations that evaluate the equipment capital costs. With sizing factors ranging from 0.4 to 0.7, these sizing equations are actually separable concave functions. An MINLP problem with separable concave functions in the objective function can be effectively handled by a branch-and-refine algorithm.[78−80] We present a formulation for the piecewise linear approximation in constraints S392−S394 in the Supporting Information based on the properties of special ordered sets of type 2.[81−83]

$$\begin{aligned}&\min \quad obj = mtac - Q\cdot v^{diesel}\\ &\text{s. t.} \quad \text{original constraints S1}-\text{S391}\\ &\qquad mgwp \le \varepsilon\cdot t\end{aligned} \tag{P3}$$

$$\begin{aligned}&\min \quad obj = mtac - Q\cdot v^{diesel}\\ &\text{s. t.} \quad \text{original constraints S1}-\text{S317, S319}-\text{S391}\\ &\qquad mgwp \le \varepsilon\cdot t\\ &\qquad \text{piecewise linear approximation functions S392}-\text{S394}\end{aligned} \tag{P4}$$

For the model P2, the additional presence of a fractional term in the economic objective function leads to more computation challenges. In this work, the parametric algorithm dedicated to solving problems with fractional terms is applied and integrated with the branch-and-refine algorithm.[24] In the parametric algorithm, we introduce a parameter Q and replace the objective function with obj as in problem P3. Consequentially, Newton's method can be applied to search for the optimal objective function value of P2 that has been illustrated by a number of successful applications of solving large-scale, complex mixed-integer fractional programming problems.[84−88] Regarding the remaining nonlinear terms in P3, we formulate a relaxed, mixed-integer linear programming (MILP) problem P4 using the proposed piecewise linear approximation. As a result, the optimal objective function value of P4 underestimates that of P3, but gradually approaches it when the accuracy of the approximation functions increases. To properly implement the two algorithms, a global optimization strategy is employed whose pseudocode is shown in Figure 10. The outer loop implements the

Global Optimization Strategy

Set $Q = 0$, $Iter^{out} = 1$, $obj = +\infty$
While $obj \ge TOL^{out}$
  Set $LB^G = 0$, $UB^G = +\infty$, $Iter^{in} = 1$, $GAP = +\infty$
  Initialize problem (P2) with two insertion points
  While $GAP \ge TOL^{in}$
    Solve problem (P2), and obtain optimal solution x^* and optimal objective function value obj^*
    Evaluate the original objective function with x^*, and obtain obj^{Δ}
    Reconstruct relaxed problem (P2) by adding x^* as a new partition point
    Set $LB^G = \max\{LB^G, obj^*\}$, $UB^G = \min\{UB^G, obj^{\Delta}\}$, $GAP = 1 - LB^G / UB^G$, $Iter^{in} = Iter^{in} + 1$
  end while
  Update $Q = \frac{mtac^*}{v^{diesel,*}}$, $Iter^{out} = Iter^{out} + 1$
end while
Return Q

Figure 10. Pseudocode of the global optimization strategy.

parametric algorithm based on Newton's method, while the inner loop implements the branch-and-refine algorithm based on successive piecewise linear approximations to ensure the relaxed formulation achieves enough approximation accuracy. $Iter^{out}$ and $Iter^{in}$ are the iteration counters for the outer loop and inner loop, respectively. The absolute optimality tolerances for the outer loop and inner loop are denoted as TOL^{out} and TOL^{in}, respectively. The current upper bounds and lower bounds are denoted as LB^G and UB^G, respectively. The initial values of obj and GAP are set to $+\infty$. Thus, this nonconvex MINLP problem can be solved by using only an MILP solver.[74]

RESULTS AND DISCUSSION

All the computational experiments are conducted on a Dell Optiplex 790 desktop with Intel(R) Core(TM) i5-2400 3.10GHz CPU, 8GB RAM and Windows 7 64-bit operating system. All the models are coded in GAMS 24.3.1.[59] Specifically, the MILP solver employed is CPLEX 12.6, while the MINLP solvers utilized are BARON 14.0,[89] and SCIP 3.1. The relative optimality tolerances of BARON 14.0 and SCIP 3.1, and the absolute optimality tolerances for both the parametric algorithm and the branch-and-refine algorithm are all set to 10^{-6}.

Environmental Life Cycle Analysis and Optimization Results for Manufacturing Bioproducts and Biodiesel from Microalgae. In this section, we present the life cycle environmental performance of producing biodiesel and each type of bioproduct from microalgae, and compare the optimization results with the results from the literature.

If the bioproduct manufacturing section is devoted to hydrogen production, the lowest unit GWP obtained is 4.28 kg CO_2-eq/kg H_2 and the corresponding optimal process selects pressure filtration in the Harvesting section, hexane as the lipid extractant, direct combustion for biogas utilization, enzyme-catalyzed transesterification for biofuel production, and glycerol steam reforming to produce hydrogen. The life cycle environmental impacts of hydrogen production has been studied by several researchers, and the unit GWP ranges approximately from 1 to 12 kg CO_2-eq/kg H_2, as shown in Table 2. Hydrogen

Table 2. Life Cycle CO_2 Equivalent Emissions from Hydrogen Production

hydrogen production method	GWP (kg CO_2-eq/kg H_2)	source
steam reforming of CH_4	11.59	literature[90]
total autocatalytic decomposition of CH_4	1.10	
electrolysis cell with renewable energy sources	2.54	literature[91]
steam reforming of glycerol	4.28	this work

production by steam reforming of glycerol demonstrates significant environmental advantages over the traditional fossil-based method, reaching a life cycle GHG reduction of over 63% of the total CO_2 equivalent emissions. Although autocatalytic decomposition and electrolysis exhibit even lower unit GWP, these methods lack technological readiness and tend to be less cost-effective at a large scale.

If we fix PG as the only bioproduct produced, the minimum unit GWP is shown in Figure 11 along with environmental impact evaluation results from industry. We note that petroleum-based PG production contributes as much as 3.75 kg CO_2-eq life cycle emissions per kg of PG produced. Two commercialized biobased process from ADM(R) and Zemea(R) manage to reduce the unit GWP to 86.4% and 58.1% of the environmental impact of the petroleum-based counterpart.[92,93] Benefiting from

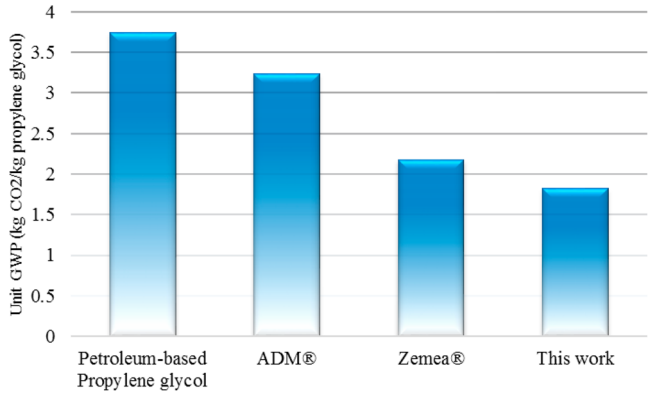

Figure 11. Life cycle CO_2 equivalent emissions from PG production.

the environmentally sustainable algal biodiesel conversion process, the unit GWP of 1.82 kg CO_2-eq/kg glycerol-based PG in this research achieves a 51.5% GHG reduction by selecting a similar upstream process configuration to the environmentally optimal process for hydrogen production.

Very little attention has been drawn to the LCA of glycerol ether products. Beatrice et al. conducted a preliminary LCA on the etherification of glycerol with *tert*-butyl alcohol and isobutylene, but sparse details were reported with respect to the specific life cycle GHG emissions of their GE's.[94] After optimizing the bioproduct process focusing on GE synthesis, we obtain a unit GWP of 2.37 kg CO_2-eq/kg GE produced. We are confident that the corresponding optimal process, which selects the same upstream processes as in the previous scenarios will be environmentally attractive and worthy of investment.

For the case of PHB production, the optimal unit GWP is 4.10 kg CO_2-eq/kg PHB with the same upstream process configuration mentioned in the above three bioproduct production scenarios. In contrast, Rostkowski et al. reported a unit GWP of 942 kg CO_2-eq/kg PHB produced from waste biogas.[61] The environmental performance of producing polyhydroxyalkanoates from corn-based PHA fermentation and recovery by Kim et al. fell in the range of 1.6−4.1 kg CO_2-eq/kg PHA.[95] In terms of the fossil based products, polypropylene, low density polyethylene, and high impact polystyrene were studied, resulting in unit GWP's of 4.34, 3.88, and 6.89 kg CO_2-eq/kg plastic, respectively.[96] Through a comparison with these literature data, it is apparent that PHB production from algal glycerol is environmentally competitive.

In terms of diesel production, the unit GWP's of producting petroleum-based diesel and soy-derived biodiesel are 0.12 and 0.025 kg CO_2-eq/MJ diesel, respectively.[64] In the current work, the production of bioproducts and biodiesel results in a minimum unit GWP of 0.040 CO_2-eq/MJ biodiesel, which can be considered at least equally environmentally sustainable to other biomass-based diesel products, and outperforms the life cycle environmental impacts of manufacturing fossil-based products. Accordingly, the environmental impact breakdown is shown in Figure 12. The manufacturing stage stands out to be the largest contributor to GWP. Specifically, the gas emissions from algae cultivation account for more than 95% of the GWP in this category and heavily affect the environmental impacts of the entire process. In the mass balance constraints, we assume the carbon dioxide utilization efficiency to be 75%, which is a conservative approximation mentioned by Frank

dx.doi.org/10.1021/sc500683w | ACS Sustainable Chem. Eng. 2015, 3, 82−96

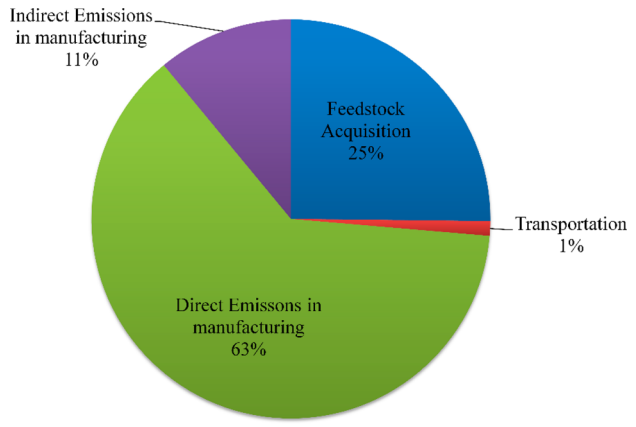

Figure 12. Total GWP breakdown for the minimum unit GWP of biodiesel.

and co-workers.[30] Therefore, an advanced cultivation system fostering a robust and efficient algal strain and enabling an improvement of the carbon utilization efficiency, could substantially reduce GHG emissions.

From the above results, bioproducts and biodiesel production from the proposed superstructure proves to be environmentally sustainable, especially compared to fossil-based chemical products. The excellent performance stems primarily from two reasons. First, when biogas derived from lipid extracted biomass is chosen to generate electricity and reusable off-gas, there is a significant reduction in GWP from selling surplus electricity, and the total environmental impacts also benefit from fewer direct GHG emissions. Second, the unit GWP is calculated to take into account coproduct allocation, averaging the environmental benefit of the entire process and further reducing the unit environmental impacts.

Economic Savings for Biofuel Production. In the existing literature, reported costs for algal biodiesel production do not align with the goal of cost-competitive biofuels.[16,20,24] The unit production cost in this work, however, is substantially reduced by producing value-added bioproduct alongside biodiesel from microalgae. Before further conclusions are drawn, a multiobjective MINLP model is solved to minimize unit biodiesel production cost and unit GWP simultaneously, and a Pareto-optimal profile is generated with the global optimization strategy and the ε-constraint method. As shown in Figure 13, the Pareto-optimal profile separates the plane into a suboptimal region and an infeasible region. Overall, the curve demonstrates the trade-off between two competing objective functions: that is, the minimum unit annualized cost (UAC) decreases when the corresponding minimum unit GWP increases. Also, the UAC drops significantly between points 3 and 4, indicating that the UAC is sensitive to certain changes in technology selections.

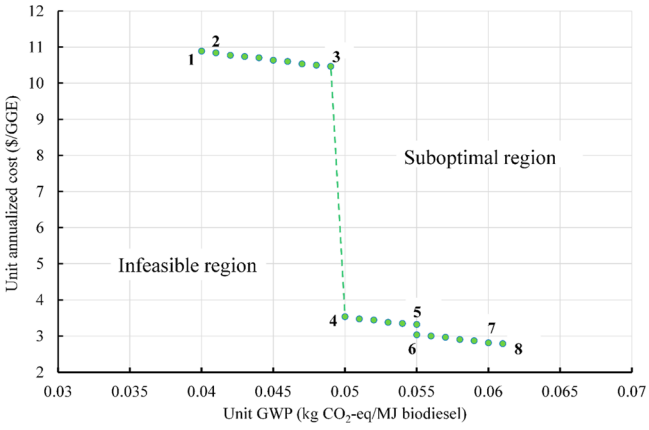

Figure 13. Pareto-optimal curve associated with the UAC and unit GWP.

With no technology presented in the cell disruption and hydrogen production sections, the most environmentally sustainable process selected by point 1 employs pressure filtration in the Harvesting section, hexane as the lipid extractant, direct combustion for biogas utilization, enzyme-catalyzed transesterification for biofuel production, and GE synthesis for bioproduct manufacturing. The minimum unit GWP of this process is 0.040 kg CO_2-eq/MJ biodiesel, but we must shoulder a UAC of $10.89/GGE in exchange for the environmental savings. In contrast, the optimal process for points 4 to 5 (Figure 14) favors supercritical carbon dioxide in the Lipid Extraction section. As mentioned previously, the selection of this technology could lead to considerable unit cost reduction, but gently impact the environment. Eventually, the optimal process selected by point 8 achieves a UAC of $2.79/GGE and a unit GWP of 0.061 kg CO_2-eq/MJ biodiesel by using centrifugation and heterogeneously catalyzed transesterification. Overall, this result has a 74% decrease in UAC with a 34% increase in GWP, which shows that significantly larger savings in UAC can be obtained than the increase in unit GWP.

The optimal economic and environmental performance on the Pareto-optimal curve depends not only on technology selection but also on the strategy to satisfy utility consumption. Points 2 and 3 select the same process configuration, but differ in the amount of natural gas purchased for steam generation. If heat consumption is satisfied by burning natural gas, a large proportion of the resulting off-gas can be reused and the environmental impact associated with the heat should be much lower than that of purchased steam. However, equipment construction for the steam generation system is costly, so as more heat is generated on site, the less economically viable a process will be.

The economic and environmental performances, as well as the throughputs of the four extreme points, corresponding to minimum total GWP, minimum total cost, minimum unit GWP, and minimum unit cost are presented in Table 3. From the Pareto-optimal point of view, the first two solutions locate in the suboptimal region and represent two feasible but nonoptimal solutions. Note that the UAC is defined as the ratio of the modified TAC to the biodiesel throughput, which should be different from the ratio of TAC to the throughput. Similarly, when we calculate the unit GWP, the environmental impact allocation of coproducts are taken into consideration to isolate the contribution caused solely by the biodiesel product. According to the U.S. Department of Energy,[97] the biodiesel price in April, 2014 was $4.01/gallon, or $4.18/GGE. From the Pareto-optimal curve, the optimal biodiesel production costs for the strategy of coproduction of bioproducts outlined in this work, ranging from $3.54/GGE and $2.79/GGE for points 4 to 8, are cost-competitive.

Computational Results. In this subsection, we compare the computation performances of the four extreme points, solved by BARON 14.0,[89] SCIP 3.1, and the proposed global optimization strategy. The model of minimizing the UAC by BARON 14.0[89] and SCIP 3.1 consists of 23 discrete variables,

dx.doi.org/10.1021/sc500683w | ACS Sustainable Chem. Eng. 2015, 3, 82−96

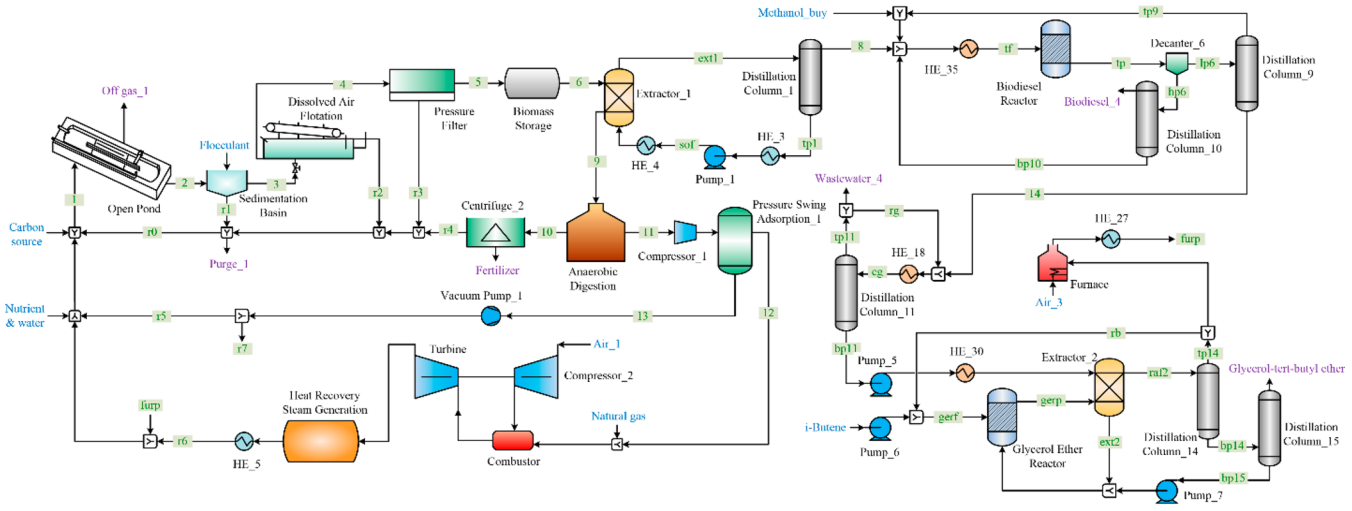

Figure 14. Optimal process flow diagram of point 4.

Table 3. Performances of Four Extreme Points[a]

	minimum total GWP	minimum TAC	minimum unit GWP	minimum UAC
TAC ($MM)	224.07	***207.04***	289.29	240.56
total GWP (kt CO_2-eq)	***1011.25***	1052.12	1143.16	1074.59
UAC ($/GGE)	3.47	3.35	10.85	***2.79***
unit GWP (kg CO_2-eq/MJ biodiesel)	0.064	0.075	***0.040***	0.061
biodiesel throughput (million GGE)	48.07	47.27	***18.73***	47.39

[a]The minimum value in each row is highlighted in bold and italic.

Table 4. Computation Comparison for Four Extreme Points on the Pareto-Optimal Curves

	BARON 14.0[89]		SCIP 3.1		proposed solution methods		
objective function	optimal value	CPU(s)	optimal value	CPU(s)	optimal value	CPU(s)	Iter
total GWP (kt CO_2-eq)	1011.25	3.37	1011.25	0.32	1011.25	0.25	1
TAC ($MM)	207.04	290	207.04	4.52	207.04	19.34	6
unit GWP (kg CO_2-eq/MJ biodiesel)	0.04	3435	NA[a]	3600	0.04	0.92	4
UAC ($/GGE)	2.79	3275	2.79	23.33	2.79	11.06	5−5[b]

[a]The calculation is terminated with "intermediate infeasible". A lower bound of 0.012 is returned. [b]This point is solved with two outer iterations by parametric algorithm, costing five inner iterations each.

9185 continuous variables, and 9801 constraints, whereas the number of continuous variables and constraints slightly increases when the problem is solved by the proposed global optimization strategy.

As listed in Table 4, the problem of minimizing total GWP can be readily solved by all three methods because this problem is simply an MILP. In the remaining cases, BARON 14.0[89] is able to provide global optimal solutions in longer computation times. In contrast, the proposed solution methods are able to obtain optimal solutions in seconds. SCIP 3.1 is efficient when solving problems with economic objective functions, but is unable to provide optimal information for the unit GWP problem within 3600 s. Overall, the proposed solution methods could considerably improve computation efficiency when globally optimizing problems with separable concave terms, or together with a fractional term in the objective function. For a similar nonconvex problem with a much larger size, general purpose solvers would hardly be able to return global optimal solutions in reasonable computation times, whereas the proposed method solves only linear problems during each iteration and still holds promise to obtain feasible solutions close to the global optimality.

CONCLUSION

In this paper, we proposed by far the most comprehensive superstructure for the production of biodiesel and four bioproducts, including hydrogen, PG, GE, and PHB from microalgae. On the basis of the proposed superstructure, we conducted a cradle-to-gate LCA and developed a bicriteria MINLP model to simultaneously optimize the environmental and economic performance following the life cycle optimization framework. The computation efficiency was enhanced with a tailored global optimization strategy. In terms of the environmental impacts, manufacturing algal bioproducts resulted in reduction of unit life cycle GHG emissions by 5% to 63%, compared with the petrochemical counterparts. The coproduction of value-added bioproducts from algal glycerol helped reduce the biodiesel production cost to as low as $2.79/GGE by employing centrifugation in the Harvesting section, supercritical carbon dioxide as the lipid extractant, direct combustion for biogas utilization, heterogeneously catalyzed transesterification for biofuel production, and GE synthesis in bioproduct production. Computational results show that the tailored solution methods can significantly reduce the computational times of solving the proposed nonconvex MINLP problems.

dx.doi.org/10.1021/sc500683w | ACS Sustainable Chem. Eng. 2015, 3, 82−96

■ ASSOCIATED CONTENT

Supporting Information

Aspen Plus simulation screenshots for two lipid extraction processes, detailed data tables, complete mathematical model formulation, and notations used in the model are included. This material is available free of charge via the Internet at http://pubs.acs.org.

■ AUTHOR INFORMATION

Corresponding Author

*F. You. Phone: (847) 467-2943. Fax: (847) 491-3728. E-mail: you@northwestern.edu.

Notes

The authors declare no competing financial interest.

■ ACKNOWLEDGMENTS

We gratefully acknowledge the financial support from the Institute for Sustainability and Energy at Northwestern University (ISEN).

■ REFERENCES

(1) Dalgaard, T.; Jorgensen, U.; Olesen, J. E.; Jensen, E. S.; Kristensen, E. S. Looking at biofuels and bioenergy. *Science* **2006**, *312* (5781), 1743−1743.

(2) Dodds, D. R.; Gross, R. A. Chemcials from Biomass. *Science* **2007**, *318*, 1250−1251.

(3) Yue, D. J.; You, F. Q.; Snyder, S. W. Biomass-to-bioenergy and biofuel supply chain optimization: Overview, key issues and challenges. *Comput. Chem. Eng.* **2014**, *66*, 36−56.

(4) Lipinsky, E. S. Chemicals from biomass: Petrochemical substitution options. *Science* **1981**, *212* (4502), 1465−1471.

(5) Bozell, J. J.; Petersen, G. R. Technology development for the production of biobased products from biorefinery carbohydrates—The US Department of Energy's "top 10" revisited. *Green Chem.* **2010**, *12* (4), 539−554.

(6) Haveren, J. v.; Scott, E. L.; Sanders, J. Bulk chemicals from biomass. *Biofuels, Bioprod. Biorefin.* **2008**, *2* (1), 41−57.

(7) Perlack, R. D.; Wright, L. L.; Turhollow, A. F.; Graham, R. L.; Stokes, B. J.; Erbach, D. C. *Biomass as feedstock for a bioenergy and bioproducts industry: The technical feasibility of a billion-ton annual supply*; Report No. DOE/GO-102005-2135; Oak Ridge National Laboratory: Oak Ridge, TN, 2005.

(8) Regalbuto, J. An NSF perspective on next generation hydrocarbon biorefineries. *Comput. Chem. Eng.* **2010**, *34* (9), 1393−1396.

(9) Gallezot, P. Conversion of biomass to selected chemical products. *Chem. Soc. Rev.* **2012**, *41* (4), 1538−1558.

(10) Werpy, T.; Petersen, G.; Aden, A.; Bozell, J.; Holladay, J.; White, J.; Manheim, A.; Eliot, D.; Lasure, L.; Jones, S. *Top value added chemicals from biomass. Volume 1—Results of screening for potential candidates from sugars and synthesis gas*; Report No. DOE/GO-102004-1992; National Renewable Energy Laboratory: Washington, DC, 2004.

(11) Pagliaro, M.; Ciriminna, R.; Kimura, H.; Rossi, M.; Della Pina, C. From glycerol to value-added products. *Angew. Chem., Int. Ed.* **2007**, *46* (24), 4434−4440.

(12) Zhou, C. H.; Zhao, H.; Tong, D. S.; Wu, L. M.; Yu, W. H. Recent advances in catalytic conversion of glycerol. *Catal. Rev.: Sci. Eng.* **2013**, *55* (4), 369−453.

(13) Bollmeier, W.; Sprague, S.; No, F. *Aquatic species program annual report*; Solar Energy Research Institute: Golden, CO, 1989.

(14) Davis, R.; Aden, A. *Renewable diesel from algal lipids: An integrated baseline for cost, emissions, and resource potential from a harmonized model*; Argonne National Laboratory: Argonne, IL, 2012.

(15) Gebreslassie, B. H.; Waymire, R.; You, F. Sustainable design and synthesis of algae-based biorefinery for simultaneous hydrocarbon biofuel production and carbon sequestration. *AIChE J.* **2013**, *59* (5), 1599−1621.

(16) Gong, J.; You, F. Q. Optimal design and synthesis of algal biorefinery processes for biological carbon sequestration and utilization with zero direct greenhouse gas emissions: MINLP model and global optimization algorithm. *Ind. Eng. Chem. Res.* **2014**, *53* (4), 1563−1579.

(17) Martin, M.; Grossmann, I. E. Simultaneous optimization and heat integration for the coproduction of diesel substitutes: Biodiesel (FAME and FAEE) and glycerol ethers from algae oil. *Ind. Eng. Chem. Res.* **2014**, *53* (28), 11371−11383.

(18) Rizwan, M.; Lee, J. H.; Gani, R. Optimal processing pathway for the production of biodiesel from microalgal biomass: A superstructure based approach. *Comput. Chem. Eng.* **2013**, *58*, 305−314.

(19) Gutierrez-Arriaga, C. G.; Serna-Gonzalez, M.; Ponce-Ortega, J. M.; El-Halwagi, M. M. Sustainable integration of algal biodiesel production with steam electric power plants for greenhouse gas mitigation. *ACS Sustainable Chem. Eng.* **2014**, *2* (6), 1388−1403.

(20) Silva, C.; Soliman, E.; Cameron, G.; Fabiano, L. A.; Seider, W. D.; Dunlop, E. H.; Coaldrake, A. K. Commercial-scale biodiesel production from algae. *Ind. Eng. Chem. Res.* **2013**, *53* (13), 5311−5324.

(21) Pokoo-Aikins, G.; Nadim, A.; El-Halwagi, M. M.; Mahalec, V. Design and analysis of biodiesel production from algae grown through carbon sequestration. *Clean Technol. Environ. Policy* **2010**, *12* (3), 239−254.

(22) Wang, B.; Gebreslassie, B. H.; You, F. Q. Sustainable design and synthesis of hydrocarbon biorefinery via gasification pathway: Integrated life cycle assessment and technoeconomic analysis with multiobjective superstructure optimization. *Comput. Chem. Eng.* **2013**, *52*, 55−76.

(23) Zhang, Q.; Gong, J.; Skwarczek, M.; Yue, D.; You, F. Sustainable process design and synthesis of hydrocarbon biorefinery through fast pyrolysis and hydroprocessing. *AIChE J.* **2014**, *60* (3), 980−994.

(24) Gong, J.; You, F. Global optimization for sustainable design and synthesis of algae processing network for CO_2 mitigation and biofuel production using life cycle optimization. *AIChE J.* **2014**, *60* (9), 3195−3210.

(25) Gebreslassie, B. H.; Slivinsky, M.; Wang, B. L.; You, F. Q. Life cycle optimization for sustainable design and operations of hydrocarbon biorefinery via fast pyrolysis, hydrotreating and hydrocracking. *Comput. Chem. Eng.* **2013**, *50*, 71−91.

(26) Lira-Barragán, L. F.; Ponce-Ortega, J. M.; Serna-González, M.; El-Halwagi, M. M. Optimal design of process energy systems integrating sustainable considerations. *Energy* **2014**, *76*, 139−160.

(27) He, C.; You, F.; Feng, X. A novel hybrid feedstock to liquids and electricity process: Process modeling and exergoeconomic life cycle optimization. *AIChE J.* **2014**, *60* (11), 3739−3753.

(28) Grossmann, I. E. Mixed-integer nonlinear programming techniques for the synthesis of engineering systems. *Res. Eng. Des.* **1990**, *1* (3−4), 205−228.

(29) Hanagata, N.; Takeuchi, T.; Fukuju, Y.; Barnes, D. J.; Karube, I. Tolerance of Microalgae to High CO_2 and High-Temperature. *Phytochemistry* **1992**, *31* (10), 3345−3348.

(30) Frank, E.; Han, J.; Palou-Rivera, I.; Elgowainy, A.; Wang, M. *Life-cycle analysis of algal lipid fuels with the greet model*; Center for Transportation Research, Energy Systems Division; Argonne National Laboratory: Oak Ridge, TN, 2011.

(31) California Stormwater Quality Association. *California Stormwater BMP Handbook-New Development and Redevelopment*; California Stormwater Quality Association: Menlo Park, CA, 2003.

(32) Granados, M. R.; Acien, F. G.; Gomez, C.; Fernandez-Sevilla, J. M.; Grima, E. M. Evaluation of flocculants for the recovery of freshwater microalgae. *Bioresour. Technol.* **2012**, *118*, 102−110.

(33) Davis, R.; Aden, A.; Pienkos, P. T. Techno-economic analysis of autotrophic microalgae for fuel production. *Appl. Energy* **2011**, *88* (10), 3524−3531.

(34) Wang, L. K.; Shammas, N. K.; Hung, Y. T. *Biosolids Treatment Processes*, Vol. *6*; Humana Press: New York, 2007.

(35) Uduman, N.; Qi, Y.; Danquah, M. K.; Forde, G. M.; Hoadley, A. Dewatering of microalgal cultures: A major bottleneck to algae-based fuels. *J. Renewable Sustainable Energy* **2010**, *2* (1), 012701.
(36) Lee, J. Y.; Yoo, C.; Jun, S. Y.; Ahn, C. Y.; Oh, H. M. Comparison of several methods for effective lipid extraction from microalgae. *Bioresour. Technol.* **2010**, *101*, S75−S77.
(37) Halim, R.; Danquah, M. K.; Webley, P. A. Extraction of oil from microalgae for biodiesel production: A review. *Biotechnol. Adv.* **2012**, *30* (3), 709−732.
(38) Plus, A. Aspen Plus user guide; Aspen Technology Limited: Cambridge, MA, 2003.
(39) Smith, R. L.; Inomata, H.; Kanno, M.; Arai, K. Energy analysis of supercritical carbon dioxide extraction processes. *J. Supercrit. Fluids* **1999**, *15* (2), 145−156.
(40) Bravi, M.; Bubbico, R.; Manna, F.; Verdone, N. Process optimization in sunflower oil extraction by supercritical CO_2. *Chem. Eng. Sci.* **2002**, *57* (14), 2753−2764.
(41) Ma, F. R.; Hanna, M. A. Biodiesel production: A review. *Bioresour. Technol.* **1999**, *70* (1), 1−15.
(42) Meher, L. C.; Sagar, D. V.; Naik, S. N. Technical aspects of biodiesel production by transesterification - A review. *Renewable Sustainable Energy Rev.* **2006**, *10* (3), 248−268.
(43) Apostolakou, A. A.; Kookos, I. K.; Marazioti, C.; Angelopoulos, K. C. Techno-economic analysis of a biodiesel production process from vegetable oils. *Fuel Process. Technol.* **2009**, *90* (7−8), 1023−1031.
(44) West, A. H.; Posarac, D.; Ellis, N. Assessment of four biodiesel production processes using HYSYS. Plant. *Bioresour. Technol.* **2008**, *99* (14), 6587−6601.
(45) Sotoft, L. F.; Rong, B. G.; Christensen, K. V.; Norddahl, B. Process simulation and economical evaluation of enzymatic biodiesel production plant. *Bioresour. Technol.* **2010**, *101* (14), 5266−5274.
(46) Ebshish, A.; Yaakob, Z.; Taufiq-Yap, Y. H.; Bshish, A.; Tasirin, S. M. Review of hydrogen production via glycerol reforming. *Proc. Inst. Mech. Eng., Part A* **2012**, *226* (A8), 1060−1075.
(47) Jones, S. B.; Valkenburg, C.; Walton, C. W.; Elliott, D. C.; Holladay, J. E.; Stevens, D. J.; Kinchin, C.; Czernik, S. *Production of gasoline and diesel from biomass via fast pyrolysis, hydrotreating and hydrocracking: A design case*; Report No. PNNL-18284; Pacific Northwest National Laboratory: Richland, WA, 2009.
(48) Huber, G. W.; Iborra, S.; Corma, A. Synthesis of transportation fuels from biomass: Chemistry, catalysts, and engineering. *Chem. Rev.* **2006**, *106* (9), 4044−4098.
(49) Hajjaji, N.; Chahbani, A.; Khila, Z.; Pons, M. N. A comprehensive energy-exergy-based assessment and parametric study of a hydrogen production process using steam glycerol reforming. *Energy* **2014**, *64*, 473−483.
(50) Valliyappan, T.; Ferdous, D.; Bakhshi, N. N.; Dalai, A. K. Production of hydrogen and syngas via steam gasification of glycerol in a fixed-bed reactor. *Top. Catal.* **2008**, *49* (1−2), 59−67.
(51) Choi, Y.; Stenger, H. G. Water gas shift reaction kinetics and reactor modeling for fuel cell grade hydrogen. *J. Power Sources* **2003**, *124* (2), 432−439.
(52) Lin, K. H.; Chang, A. C. C.; Lin, W. H.; Chen, S. H.; Chang, C. Y.; Chang, H. F. Autothermal steam reforming of glycerol for hydrogen production over packed-bed and Pd/Ag alloy membrane reactors. *Int. J. Hydrogen Energy* **2013**, *38* (29), 12946−12952.
(53) Kooijman, H. Air separation unit with pure argon recovery (simplified). http://chemsep.org/downloads/data/CScasebook_ASU.pdf (accessed 8/18/2014).
(54) Guo, Y.; Liu, X. H.; Azmat, M. U.; Xu, W. J.; Ren, J. W.; Wang, Y. Q.; Lu, G. Z. Hydrogen production by aqueous-phase reforming of glycerol over Ni-B catalysts. *Int. J. Hydrogen Energy* **2012**, *37* (1), 227−234.
(55) Pagliaro, M.; Rossi, M. *The future of glycerol*; Royal Society of Chemistry: Cambridge, U. K., 2010.
(56) Bloom, P. Generating high purity, biobased propylene glycol; by product inhibition; reactor system. U.S. Patent 8153847 B2, April 10, 2011.
(57) Tuck, M. W. M. Process for the hydrogenation of glycerol to propylene glycol. U.S. Patent 8227646 B2, July 24, 2012.
(58) Vlad, E.; Bildea, C. S.; Bozga, G. Robust optimal design of a glycerol etherification process. *Chem. Eng. Technol.* **2013**, *36* (2), 251−258.
(59) Choi, J. I.; Lee, S. Y. Process analysis and economic evaluation for poly(3-hydroxybutyrate) production by fermentation. *Bioprocess Eng.* **1997**, *17* (6), 335−342.
(60) Posada, J. A.; Naranjo, J. M.; Lopez, J. A.; Higuita, J. C.; Cardona, C. A. Design and analysis of poly-3-hydroxybutyrate production processes from crude glycerol. *Process Biochem.* **2011**, *46* (1), 310−317.
(61) Rostkowski, K. H.; Criddle, C. S.; Lepech, M. D. Cradle-to-gate life cycle assessment for a cradle-to-cradle cycle: Biogas-to-bioplastic (and back). *Environ. Sci. Technol.* **2012**, *46* (18), 9822−9829.
(62) Plattner, G.-K.; Stocker, T.; Midgley, P.; Tignor, M. *IPCC expert meeting on the science of alternative metrics*, Oslo, Norway, March 18−20, 2009.
(63) Sander, K.; Murthy, G. S. Life cycle analysis of algae biodiesel. *Int. J. Life Cycle Assess.* **2010**, *15* (7), 704−714.
(64) Passell, H.; Dhaliwal, H.; Reno, M.; Wu, B.; Ben Amotz, A.; Ivry, E.; Gay, M.; Czartoski, T.; Laurin, L.; Ayer, N. Algae biodiesel life cycle assessment using current commercial data. *J. Environ. Manage.* **2013**, *129*, 103−111.
(65) Campbell, P. K.; Beer, T.; Batten, D. Life cycle assessment of biodiesel production from microalgae in ponds. *Bioresour. Technol.* **2011**, *102* (1), 50−56.
(66) DOT Table 6 Shipment Characteristics by Two-Digit Commodity for the Unied States; U.S. Department of Transportation: Washington, DC, 2012. http://www.rita.dot.gov/bts/sites/rita.dot.gov.bts/files/publications/commodity_flow_survey/2012/united_states/table6.html (accessed September 2014).
(67) *Ecoinvent database*, v3.1; Swiss Centre for Life Cycle Inventories: Bern, Switzerland, 2014.
(68) Seider, W. D.; Seader, J. D.; Lewin, D. R. *Product & process design principles: Synthesis, analysis and evaluation*. John Wiley & Sons: New York, 2009.
(69) Kreutz, T.; Williams, R.; Consonni, S.; Chiesa, P. Co-production of hydrogen, electricity and CO_2 from coal with commercially ready technology. Part B: Economic analysis. *Int. J. Hydrogen Energy* **2005**, *30* (7), 769−784.
(70) ISO. *Environmental management—Life cycle assessment—Principles and framework*; ISO Standard No. 14040:2006; British Standards Institution: London, 2006.
(71) You, F. Q.; Wang, B. Life cycle optimization of biomass-to-liquid supply chains with distributed-centralized processing networks. *Ind. Eng. Chem. Res.* **2011**, *50* (17), 10102−10127.
(72) You, F. Q.; Tao, L.; Graziano, D. J.; Snyder, S. W. Optimal design of sustainable cellulosic biofuel supply chains: Multiobjective optimization coupled with life cycle assessment and input-output analysis. *AIChE J.* **2012**, *58* (4), 1157−1180.
(73) Yue, D. J.; Slivinsky, M.; Sumpter, J.; You, F. Q. Sustainable design and operation of cellulosic bioelectricity supply chain networks with life cycle economic, environmental, and social optimization. *Ind. Eng. Chem. Res.* **2014**, *53* (10), 4008−4029.
(74) Yue, D. J.; Kim, M. A.; You, F. Q. Design of sustainable product systems and supply chains with life cycle optimization based on functional unit: General modeling framework, mixed-integer nonlinear programming algorithms and case study on hydrocarbon biofuels. *ACS Sustainable Chem. Eng.* **2013**, *1* (8), 1003−1014.
(75) Tong, K. L.; You, F. Q.; Rong, G. Robust design and operations of hydrocarbon biofuel supply chain integrating with existing petroleum refineries considering unit cost objective. *Comput. Chem. Eng.* **2014**, *68*, 128−139.
(76) Lardon, L.; Helias, A.; Sialve, B.; Steyer, J. P.; Bernard, O. Life-cycle assessment of biodiesel production from microalgae. *Environ. Sci. Technol.* **2009**, *43* (17), 6475−6481.
(77) Hwang, C. L.; Masud, A. S. M. *Multiple objective decision making-Methods and applications*; Springer: Berlin, 1979; Vol. *164*.

(78) You, F. Q.; Grossmann, I. E. Stochastic inventory management for tactical process planning under uncertainties: MINLP models and algorithms. *AIChE J.* **2011**, *57* (5), 1250−1277.
(79) You, F. Q.; Pinto, J. M.; Grossmann, I. E.; Megan, L. Optimal distribution-inventory planning of industrial gases. II. MINLP Models and algorithms for stochastic cases. *Ind. Eng. Chem. Res.* **2011**, *50* (5), 2928−2945.
(80) Yue, D. J.; You, F. Q. Planning and scheduling of flexible process networks under uncertainty with stochastic inventory: MINLP models and algorithm. *AIChE J.* **2013**, *59* (5), 1511−1532.
(81) Yue, D.; You, F. Game-theoretic modeling and optimization of multi-echelon supply chain design and operation under Stackelberg game and market equilibrium. *Comput. Chem. Eng.* **2014**, *71* (0), 347−361.
(82) Yue, D.; You, F. Fair profit allocation in supply chain optimization with transfer price and revenue sharing: MINLP model and algorithm for cellulosic biofuel supply chains. *AIChE J.* **2014**, *60* (9), 3211−3229.
(83) Garcia, D. J.; You, F. Multiobjective optimization of product and process networks: General modeling framework, efficient global optimization algorithm, and case studies on bioconversion. *AIChE J.* **2015**, DOI: 10.1002/aic.14666.
(84) Zhong, Z. X.; You, F. Q. Globally convergent exact and inexact parametric algorithms for solving large-scale mixed-integer fractional programs and applications in process systems engineering. *Comput. Chem. Eng.* **2014**, *61*, 90−101.
(85) You, F. Q.; Castro, P. M.; Grossmann, I. E. Dinkelbach's algorithm as an efficient method to solve a class of MINLP models for large-scale cyclic scheduling problems. *Comput. Chem. Eng.* **2009**, *33* (11), 1879−1889.
(86) Yue, D. J.; You, F. Q. Sustainable scheduling of batch processes under economic and environmental criteria with MINLP models and algorithms. *Comput. Chem. Eng.* **2013**, *54*, 44−59.
(87) Chu, Y. F.; You, F. Q. Integration of production scheduling and dynamic optimization for multi-product CSTRs: Generalized Benders decomposition coupled with global mixed-integer fractional programming. *Comput. Chem. Eng.* **2013**, *58*, 315−333.
(88) Chu, Y. F.; You, F. Q. Integration of scheduling and control with online closed-loop implementation: Fast computational strategy and large-scale global optimization algorithm. *Comput. Chem. Eng.* **2012**, *47*, 248−268.
(89) Tawarmalani, M.; Sahinidis, N. V. A polyhedral branch-and-cut approach to global optimization. *Math. Program.* **2005**, *103* (2), 225−249.
(90) Dufour, J.; Serrano, D. P.; Galvez, J. L.; Moreno, J.; Garcia, C. Life cycle assessment of processes for hydrogen production. Environmental feasibility and reduction of greenhouse gases emissions. *Int. J. Hydrogen Energy* **2009**, *34* (3), 1370−1376.
(91) Koroneos, C.; Dompros, A.; Roumbas, G.; Moussiopoulos, N. Life cycle assessment of hydrogen fuel production processes. *Int. J. Hydrogen Energy* **2004**, *29* (14), 1443−1450.
(92) ADM life cycle analysis. http://www.adm.com/en-US/products/evolution/Propylene-Glycol/Pages/Life_Cycle_Analysis.aspx (accessed September 2014).
(93) Zemea purity and renewable performance. http://www.duponttateandlyle.com/sites/default/files/ZemeaHI%26I_lifeCycleAnalysis.pdf (accessed September 2014).
(94) Beatrice, C.; Di Blasio, G.; Lazzaro, M.; Cannilla, C.; Bonura, G.; Frusteri, F.; Asdrubali, F.; Baldinelli, G.; Presciutti, A.; Fantozzi, F.; Bidini, G.; Bartocci, P. Technologies for energetic exploitation of biodiesel chain derived glycerol: Oxy-fuels production by catalytic conversion. *Appl. Energy* **2013**, *102*, 63−71.
(95) Kim, S.; Dale, B. E. Life cycle assessment study of biopolymers (Polyhydroxyalkanoates) derived from no-tilled corn. *Int. J. Life Cycle Assess.* **2005**, *10* (3), 200−210.
(96) Roes, A.; Pietrini, M.; Chiellini, E.; Patel, M. Environmental life cycle studies of poly (hydroxybutyrate)-and polypropylene-based composites. *J. Nanostruct. Polym. Nanocompos.* **2007**, *3* (1), 22−32.
(97) DOE fuel prices. http://www.afdc.energy.gov/fuels/prices.html (accessed September 2014).